Osteoarthritis and Cartilage 18 (2010) S106–S112

Osteoarthritis and Cartilage

Cartilage, bone and synovial histomorphometry in animal models of osteoarthritis

P.C Pastoureau*, E.B Hunziker, J.-P. Pelletier

Institut de Recherches Servier, Prospective et Valorisation Scientifiques, 11 rue des Moulineaux, 92150 Suresnes, France

ARTICLE INFO

Article history:
Received 12 May 2010
Accepted 12 May 2010

Keywords:
Bone
Cartilage
Cartilage fissure
Cartilage thickness
Chondrocyte density and size
Goldner's trichrome
Histology
Histomorphometry
Image analysis
Proteoglycan content
Safranin O
Subchondral bone plate thickness
Synovium

SUMMARY

Objective: This review focuses on histomorphometry for assessing the pathological changes in various compartments of the joint including cartilage, bone and synovium in animal models of osteoarthritis (OA).
Methods: Different methodological approaches are presented concerning sampling, embedding, sectioning, staining, mounting of stained sections and measurement of histomorphometric parameters using automated and semi-automated methods. Notes are provided describing some methods in greater detail.
Results: Histomorphometry allows a significant gain of objectivity, accuracy and reproducibility in the quantification of the main histological parameters which best characterize OA in the affected joint (cartilage thickness (CT), chondrocyte size and density, cartilage fissure, proteoglycan (PG) content, subchondral bone plate thickness (SBPT), thickness of synovial living cell layer) in animal models.
Conclusion: Use of histomorphometry could contribute to a better quantification of histological differences between control and OA animals. Contributing also to the introduction of normative data, it is a major advantage for therapeutic assessments in experimental OA and particularly for the analytical comparison of the efficacy of disease modifying OA drugs (DMOAD).

Introduction

Osteoarthritis (OA) is a major joint disease of humans and various animals in which articular cartilage degenerates over a period of time causing eburnation of the joint surface. It is also characterized by concomitant changes in subchondral bone which are well documented, both in animals and in humans[1–3].

In animal models of OA, the histological assessment of articulations is the best way to properly analyze all the characteristic lesions of the disease at the cartilage and bone levels. It is mainly based on scoring evaluation and this has been largely documented in this book for the different animal models of OA (chapters 2–8). However a subjective scoring system can only be semi-quantitative and the possibility for substantial inter- and/or intra-observer variability is a concern. **Histomorphometry** with its greater degree of objectivity, accuracy and reproducibility is more appropriate. It can be defined as the quantitative structural analysis of histological parameters of three-dimensional (3D) biological structures which have been clearly defined by the investigator. It is also the process which allows measurements from two-dimensional (2D) sections defined by the laws of stereology. Hunziker recently described the basic principles that must be respected for an unbiased estimation of 3D cartilage structures and examined practical methods that are currently employed to estimate the more commonly determined parameters such as volume, surface area and number[4].

Before starting a quantitative structural analysis, the parameter to be measured must be clearly defined and must be, before all, biologically meaningful. From this, different and successive methodological steps should be respected in order to properly achieve the corresponding measurements.

This chapter first presents these different methodological steps which should allow the investigator to perform histomorphometry on articular samples obtained from a given animal model of OA. Then, as a follow-up of a previous paper[5] various histomorphometric parameters will be "re-introduced", expressing the OA pathology both at the cartilage and the bone level. Notes are provided all along the paragraphs to illustrate some technical aspects and quantified parameters obtained in an example animal model of OA.

Methodological approaches

The strength of these analytical methods is extremely dependent on the good reproducibility of measurements which also

* Address correspondence and reprint requests to: Philippe Pastoureau, Institut de Recherches Servier, Prospective et Valorisation Scientifiques, 11 rue des Moulineaux, 92150 Suresnes, France, Tel: 33 1-55-72-27-60; Fax: 33-1-55-72-27-37.
E-mail address: philippe.pastoureau@fr.netgrs.com (P.C Pastoureau).

1063-4584/$ – see front matter
doi:10.1016/j.joca.2010.05.024

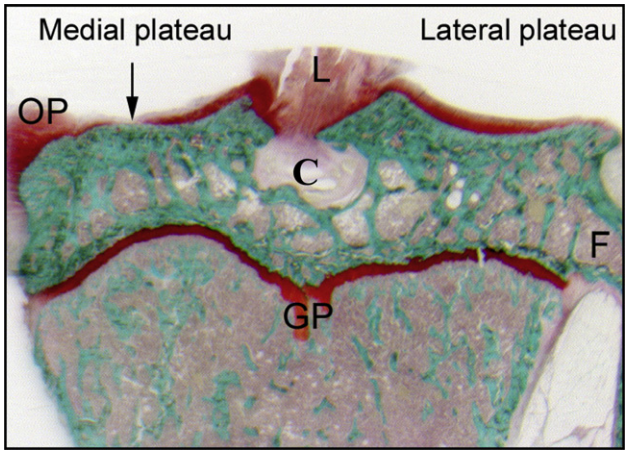

Fig. 1. Left operated proximal tibia of a MNX guinea pig. Site of measurement of histomorphometric parameters: medial tibial plateau (arrow). Safranin O staining. L = ligament. C = cavitation. GP = growth plate. (magnification: ×10)[5].

results from high-quality and precision of both materials and methods employed (joint sampling, sectioning, staining and histomorphometric measurements). Thus, the entire paragraph precisely describes each methodological point in order to help the experimenter obtain the best results. For each sub-paragraph, additional details on the precise materials and methods used are included in notes numbered at the end of the manuscript and which were published elsewhere and described in greater detail[6].

An important restriction is the **number of samples** to be analyzed for each animal. For most, OA lesions only appear in one articulation (knee essentially) in which pathology has been induced (surgically/chemically) except for spontaneous models where lesions can appear at least in two symmetric articulations. Thus, in most cases, histopathologic characterization/quantification are performed in only one sample and all the histomorphometric parameters evaluated on the same sections, randomly obtained in a precise area, being representative of the whole articulation.

Sampling is a key point at the early stage of the investigation. The whole bone (tibia or femur), but not the entire articulation (knee), must be privileged because the definition of the vertical section direction and location for sectioning is facilitated and more reproducible between samples [note 1].

Type of embedding is dependent on the goal of the study. For investigators who want to analyze the disease progression combining cartilage and bone parameters assessments, undecalcified histological procedures should be favoured [note 1] because bone integrity must be preserved treating bone samples without prior decalcification. Nevertheless, if bone assessment is not essential, histomorphometry can also be performed on paraffin sections using adapted staining methods.

Sectioning is the most important and difficult process in this series of techniques. Sections (plastic or paraffin) must be entire (no alteration in cartilage and bone tissues). A compromise between thickness (6–8 μm) and integrity must be obtained to reach this goal. [note 2]. From a practical point of view, even if random sectioning is virtually impossible[4] an important and reasonable number of sections must be collected in the correct sectioning area (see at the following) in order to select at the end of the process four non consecutive good quality sections to be analyzed. An important issue is the localization for sectioning which should be precisely defined within the sample in (or close to) the lesion area. Depending on the severity (rapidity) of apparition of lesions in the animal model used, it can be useful to consider this positioning not particularly in the central part of the lesion (where cartilage rapidly disappears with no more structure to be quantified) but in the periphery where the lesion is still progressing, enabling the measurement of various parameters on the remaining structures.

Furthermore, to ensure a reproducible positioning (vertical section direction and depth for cutting) it is necessary to define morphological indicator(s) in the embedded bone. An example is presented in Fig. 1 for the meniscectomized (MNX) guinea pig model, in which tibia is sectioned along the coronal plane for optimal exposition of the central part of the medial tibial plateau where OA lesions first appear[5].

Staining and mounting of stained sections

This final step is extremely dependent on the quality of the section (thickness and integrity) and the choice of the staining depends on the type of parameter to be measured (see § "Histomorphometric parameters").

For morphological assessments (good differentiation/delineation of all cartilage and bone structures) various staining and counterstaining are proposed in the literature. Conditions of preparation of the solutions and protocols for staining (sequences and duration of incubation of sections in staining baths) should be

Table I
Cartilage, bone and synovial histomorphometric parameters measured in different animal species

	Histomorphometric parameters	Animal species [Reference]
Cartilage	CT	Rat[8–10] Guinea Pig[5,6,11] Rabbit[12–17] Cat[18] Sheep[19–21]
	CT (hyaline area vs calcified area)	Rabbit[22] Dog[23,24] Sheep[20] Horse[25]
	Cartilage area	Guinea Pig[5,6] Rabbit[13–17,26]
	Chondrocyte density	Rat[8,10] Guinea Pig[5,6] Rabbit[27,28] Sheep[21] Monkey[29]
	Chondrocyte size	Rat[8] Rabbit/Pig[27]
	Chondrocyte to matrix area ratio	Rabbit[28]
	Cartilage surface FI	Guinea Pig[5,6,11]
	Surface undulations	Rabbit[14]
	PG content	Bovine[30] Ovine[20] Rabbit[26] Guinea Pig[5,6]
Bone	SBPT	Rat[9] Guinea Pig[5,6,11] Rabbit[31,36] Dog[23,24] Ovine[19–21] Horse[25]
	Subchondral bone plate volume	Rat[32,33] Ovine[21] Dog[34]
	Subchondral trabecular bone volume	Rat[9] Guinea Pig[5,6,35] Rabbit[36] Dog[24]
	OP area	Rat[33]
Synovium	Thickness of synovial living cell layer	Rat[9] Rabbit[14]

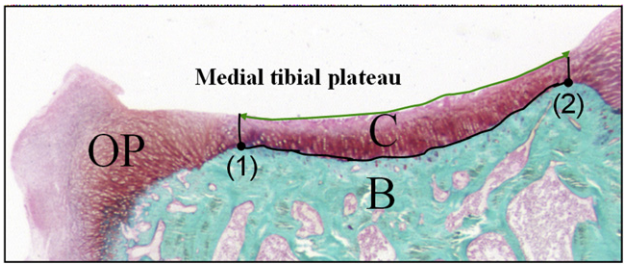

Fig. 2. Left operated tibial plateau of a MNX guinea pig. Area of measurement of the CT (in μm): automatically generated between the two manually indicated points (one and two) at the margin of cartilage (C) and bone (B). Safranin O staining. (magnification: ×20)[5].

adapted by the investigator in order to get the best differentiation for each structure. An example is provided (Goldner's trichrome) which is a "gold standard" for methacrylate embedded undecalcified 8 μm-thick sections [note 3]. This staining allows the differentiation of both calcified structures (bone and calcified cartilage) and cells (osteoblasts, osteoclasts and chondrocytes), the articular cartilage appearing as a well delineated clear structure vs bone. Safranin orange (such as alcyan blue or other specific staining for cartilage structures) clearly differentiates cartilage because it merely stains negative charged groups which best characterized proteoglycans (PG). The staining intensity can therefore be considered as proportional to the concentration of PG in the tissue, provided that no extraction occurred during processing (see § "Histomorphometric parameters", PG content section). If properly adapted [note 4], quantification (as a ratio) of PG concentration in the cartilage can be performed in the corresponding stained section (see § "Histomorphometric parameters", PG content section).

All the methodological approaches presented above are based on thick sections (6–10 μm) of which the principal disadvantage is fragility during the successive processes (sectioning, staining and mounting). As an alternative, the thick section technology elaborated by Schenk *et al.* has been used in a number of studies. This method permits the high-quality preservation of large specimens of mineralized tissue, including calcified cartilage, for histological analyses. It involves the embedment of the tissue in a plastic resin, from which thick saw cut (80–120 μm) sections are first produced, then superficially polished, and finally surface-stained with McNeal's tetrachrome, basic fuchsine and toluidine blue[7].

Histomorphometric parameters

Over the past 20 years, few studies, based on a histomorphometric evaluation of cartilage and bone lesions in animal models of OA, were published. In their majority, they concerned large animals (rabbit, cat, dog, sheep, pig, monkey and horses) because the bigger size of the samples obviously favours this evaluation. More recently, such investigations have also been performed in rats and guinea pigs. Table 1 recapitulates the various parameters which were measured in these different animal species[8–36].

Cartilage thickness (CT) is the most widely evaluated parameter in all animal species. It is probably the easiest parameter to be quantified by an automated computerized image analysis [note 5 and Fig. 2]. Furthermore CT best expresses the illness classically evoked in OA cartilage and then remains the best global histomorphometric parameter for the quantification of cartilage erosion at all stages of the disease.

CT can be evaluated over the whole width of the cartilage but also by differentiating the hyaline and the calcified areas[19,21–24].

Modifications at the cellular compartment of this tissue can also be approached by evaluating the **chondrocyte profile area density** (number of cell profiles/calcified cartilage), the **chondrocyte size** (by the point sampled intercept methodology developed by Gundersen *et al*[37]) or the real **chondrocyte to matrix area ratio**.

Fissure or surface undulations of the upper zone of the articular cartilage are also typical features of cartilage degeneration in OA. In histological applications, it has been characterized by descriptive means[34]. The technique presented in note 6, to quantitatively describe the degree of superficial fissure in the guinea pig tibial plateau, provides a means of quantifying the degree of fissure, a larger value indicating a greater degree of fissure. Measured and expressed as a Fissure index (FI; in order to normalize to the size of the measured area) in MNX guinea pig (Fig. 3), this parameter effectively and strongly discriminates between diseased and healthy animals[5].

Modifications in **PG content** during the progression of OA have been classically described[38] and quantification of these variations during the pathology process is consequently of interest. But PG, whose concentration in cartilage tissue is high, are subject to extraction when isolated blocks of cartilage are immersed within aqueous media. Even within culture media or isotonic solutions, the loss of PG lies in the order of 12–15%[39] and this value rises to between 20% and 30% when the tissue is transferred to an aldehyde-based fixative[40]. Furthermore, if this primary, aldehyde-based fixation step is followed by post-fixation in osmium tetroxide (which will be necessary if the tissue is destined for examination in the transmission electron microscope), then the accumulated loss of PG will amount to about 70% by the end of the procedure[40]. Consequently, the quality of the preservation result is highly unpredictable and variable[41,42]. The problem can be avoided by using an alternative method to chemical fixation (see "cryoprocessing" in note 7) or by precipitating the PG *in situ* with an appropriate cationic dye. This

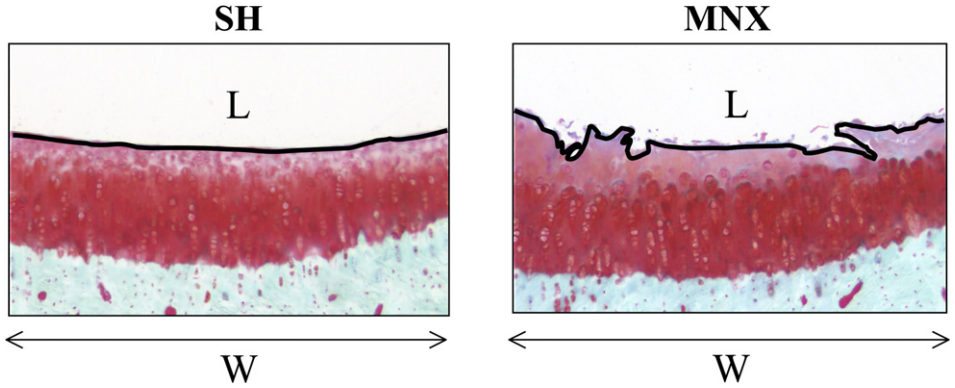

Fig. 3. Left operated tibial plateau of a sham-operated (SH) and MNX guinea pig. Measurement of the FI; automatically calculated as follows: FI = (length of upper margin of cartilage (L)/width of area of measurement (W)) x100. Safranin O staining. (magnification: ×80)[5].

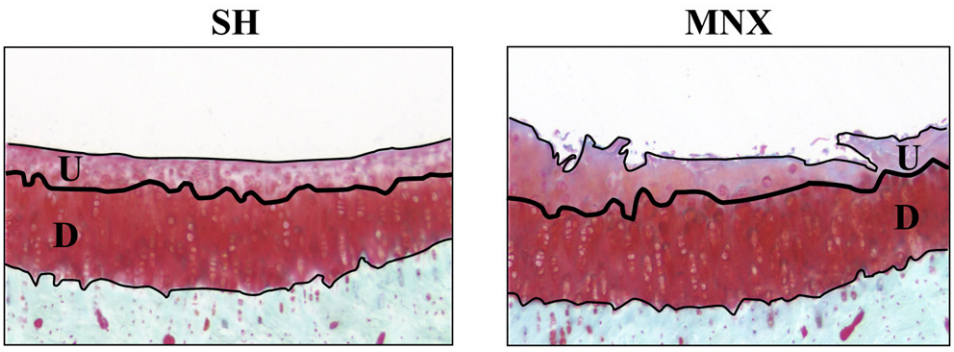

Fig. 4. Left operated tibial plateau of a SH and MNX guinea pig. Automatic measurement of the SOI in the deep (D) and upper (U) zones of the articular cartilage after manual delimitation of the D from the U zones. PGs content ratio of the cartilage is expressed as SOI in U/SOI in D. Safranin O staining. (magnification: ×80)[5].

agent must be present from the very onset of processing, as soon as the isolated block of cartilage tissue is transferred to an aqueous medium, and it should be included within each of the successive aqueous media up to the point of dehydration in ethanol[41].

Another means to bypass this issue with PG loss during chemical processing is presented in note 8. It is based on the quantification of safranin O staining intensity (SOI) using a special software and expressed as a ratio. Effectively, like for collagen content, decreased PG content is soon noticeable in the upper zone of OA cartilage whereas deep zone is subjected to enhanced PG content because of an increased synthesis by chondrocytes in this zone[43]. Thus, by evaluating SOI in the upper zone of cartilage divided by the same intensity in the deep zone (Fig. 4), the variation of quality/quantity of PG staining is minimized between sections. This was demonstrated by the good reproducibility of the measurements, allowing the detection of significant differences in the PG content ratio between OA animals and controls[5].

Although degradation of articular cartilage remains the main feature of OA, some researchers of the disease implicated the subchondral bone in exacerbating the degeneration of cartilage. In particular, Radin *et al.* speculated that increased bone mass and thickening of the subchondral bone plate may in fact be the primary event of joint degeneration and proposed that increases in stiffness of the underlying bone were associated with cartilage degeneration[1]. This apparent coupling between cartilage and bone turnover even recently resulted in the consideration that subchondral bone turnover could be targeted for treating OA[44]. Thus, the interest of measuring **subchondral bone parameters** at the histological levels is clearly emphasized. Few studies have been referenced in this field during the past 20 years but this type of measurement has been performed in the main animal models of OA (Table 1). The subchondral bone plate thickness (SBPT) is the best indicator of the bone sclerosis classically observed at the late stages of the OA disease. It has been measured in most species and an example of an automatic method is presented in note 9 and illustrated in Fig. 5. This latter method is based, as others, on the segmentation of the bone in the superior part of the epiphysis which obviously includes the subchondral bone plate. Bone volume at the subchondral (superior part of the epiphysis) or the trabecular (all the epiphysis) level can also be considered as secondary indices of bone remodelling. Osteophyte (OP) area measurement has only been performed once in the rat[32]. It characterizes a late event in the pathogenesis of OA but can be evaluated as a typical feature of this pathology particularly in animal models which are more susceptible to osteophytosis.

Changes which occur in the OA synovium are not as visually striking as those which occur in rheumatoid arthritis (RA) joints; however, this does not mean that OA synovium is normal in this pathology and particularly at the histological level. On the contrary, advanced OA is often characterized by cartilaginous fragments embedded in the synovium, resulting in more pronounced synovitis. Most of these changes have been demonstrated elsewhere by immunohistological studies on both human and animal models of OA[45]. Thus it can be interesting to quantify the **thickness of synovial living cell layer** as a marker of the degree of synovitis like in animal models of RA[9] or in response to locally administered drugs such as in rabbits[13].

Discussion

This chapter first lists the different methodological steps (sampling, embedding, sectioning, staining and mounting) which should allow the investigator to properly perform histomorphometry on articular samples obtained from various animal models of OA.

Various histomorphometric parameters are then introduced, all of them expressing the OA pathology both at the cartilage, bone and synovium levels. For most of them, the analysis can be based on an automated computerized system and some notes are provided along the paragraphs to help the investigator in the application of such a system to their own conditions. This histomorphometric system has effectively the advantages of objectivity, accuracy, repeatability and ease of use. The interest of this method has been used in the field of tissue engineering[46] and for the assessment of cartilage repair[47].

Furthermore, this automated method, published in more detail elsewhere[6] has been applied extensively in the MNX guinea pig model of OA in which all the main histological parameters reflecting OA features at the cartilage and bone levels could be easily

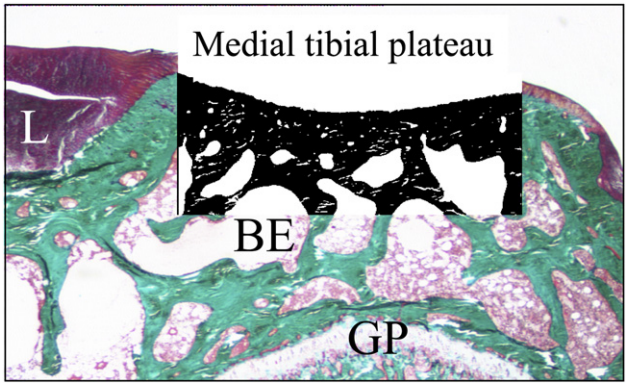

Fig. 5. Left medial tibial plateau of a guinea pig. SBPT in μm was automatically measured after segmentation of bone in the half superior part of the epiphysis (dark area). Goldner trichrome staining. L = ligament, GP = growth-plate, BE = bone epiphysis. (magnification: ×12.5)[5].

quantified and gave satisfactory results both for the OA pathological evaluation[5] and the study of a drug-modifying OA drug[48].

In general, it is also important to reemphasize that this system minimizes a large portion of the subjectivity demonstrated by previous techniques and consequently permits a more quantitative and analytical comparison between control and experimental specimens. This is a major advantage for statistical studies and particularly for those applied to the analysis of therapeutic treatments[48].

This methodology can also contribute to the introduction of normative data for the histological characterization of OA in various animal models. In those conditions, recommendations should be generated in order to normalize all the different steps of the process from sampling to measurement[4] and the resulted parameters written in a new nomenclature for expressing lesions.

Conflict of interest

No author has any conflict of interest related to this work.

Disclosures

Philippe PASTOUREAU is employed by the Institut de Recherches Servier.

Ernst HUNZIKER is employed by the University of Bern.

Jean-Pierre PELLETIER is employed by the Medical School of the University of Montreal.

Acknowledgements

No external sources of funding were provided for this work except that the printing costs were supported by an unrestricted educational grant to OARSI by Bayer, Expanscience, Genzyme, Lilly, MerckSerono, Novartis, Pfizer, SanofiAventis, Servier, and Wyeth. The work performed was not influenced at any stage by the support provided.

NOTES

Note 1

(Bone sampling and embedding):

1. Sacrifice the animals and sample tibias (from healthy or diseased joints).
2. Section the diaphysis at the insertion site of the fibula.
3. Place each bone in a flask containing the 10% formaldehyde solution for 24 h or directly in ethanol (see point four at the following).
4. Discard the formaldehyde solution and then add 80% ethanol (three successive baths of 1 week each).
5. Dehydrate in absolute ethanol (two baths of three day each).
6. Substitute ethanol with toluene for 48 h.
7. Soak with prepared MMA solutions at 4°C, for 1 week in each solution (MMA1, MMA2, and MMA3).
8. Just before embedding (in MMA3), put the tibia in the flask, with the proximal extremity at the bottom. Then place the flask with an hermetic cap in the incubator at 37°C to obtain a solid block containing the bone (for a better but slower embedding, this phase can be done more slowly, letting the solution catalyse in the flask at ambient temperature rather than 37°C).
9. Remove the block from the flask by breaking the glass with a hammer.
10. In order to take into account the focal nature of the OA process, and to be sure that all the sections are cut along the same plane, first sand each embedded tibia on a rotary abrasive disk until the right angle and location for cutting are obtained.

Note 2

(Sectioning):

1. Place and tighten the block on the microtome. The sanded surface of the block must be horizontal.
2. Start cutting at a medium speed in order to reach the desired level of sectioning.
3. Adjust the thickness of the sectioning to 8 μm and reduce the speed.
4. Slowly collect the sections using a humidified cigarette paper
5. Remove the section and place it in a glass container with distilled water.

Note 3

(Goldner's trichrome staining):

1. Put the sections in Weigert's hematoxylin solution for 10 min.
2. Rinse with running tap water and then with acetified water.
3. Place the sections in the fuchsin ponceau solution for 20 min.
4. Rinse with running tap water and acetified water.
5. Put the sections in the molybdic orange G solution for 6 min.
6. Rinse with running tap water and acetified water.
7. Place the sections in the light green solution for 15 min.
8. Rinse with running tap water and acetified water.
9. Dehydrate the sections in three consecutive baths of absolute alcohol and two baths of methylcyclohexane.
10. Mount the stained sections with a drop of mountant (Entellan) between two microscope slides and let dry (this staining results in red chondrocyte cytoplasm, black nucleus, orange matrix collagen, and green calcified cartilage and bone.)

Note 4

(Safranin O staining):

1. Put the sections in the safranin O staining solution for 10 min.
2. Rinse with running tap water.
3. Counterstain in the light green solution for 5 min.
4. Rapidly rinse with running tap water.
5. Dehydrate in two baths of absolute alcohol and one bath of methylcyclohexane.
6. Mount the stained sections with a drop of entellan mounting medium between two microscope slides and let dry (the success of this staining should result in a red or pink cartilage and green underlying bone).

Note 5

CT:

1. Use sections stained with Goldner's trichrome or Safranin O at an 80× magnification.
2. Measure the thickness between the two morphological indicators positioned as shown in Fig. 2.
3. Manually outline the cartilage area between reference marks one and two (area C in Fig. 2) and the subchondral bone.
4. The designed software should be able to segment this region of interest automatically, using, for example, a threshold for black and white extraction with a green image.
5. Calculate the thickness of cartilage as the mean length of all the segments generated from each pixel situated on the border of the corresponding cartilage area.

Note 6

FI:

1. Use sections stained with Goldner's trichrome at an 80× magnification.
2. Position the area of measurement centrally between reference marks one and two (Fig. 2).
3. The designed software must perform a segmentation of both cartilage and bone using a threshold for black and white extraction with a green image.
4. On the upper limit of the segmented area, integrate automatically the length of the superficial border (L in Fig. 3).
5. Calculate the FI by dividing L by the width (W) of the measured area (Fig. 3).

Note 7

(Cryoprocessing as an alternative to chemical fixation for PG preservation *in situ*):

As long as the cartilage tissue remains frozen, the PG will remain *in situ*. But as soon as the cryosections are thawed and exposed to an aqueous medium, which would be necessary if they are to be treated with an antibody for an immunohistochemical analysis, then the extraction of PG will begin. The losses thereby incurred will disturb the architecture of the remaining macromolecular components of the extracellular matrix, in the structural organization of which the PG are intimately involved, thereby reducing the resolution power of the subsequent immunohistochemical analysis.

Note 8

(PG content ratio):

1. Use sections stained with safranin O at an 80× magnification
2. Use the same area of measurement as for the FI (note 6)
3. Segment the cartilage automatically as for the measurement of the CT.
4. Outline the upper (U) and the deep (D) zones of the cartilage by manually drawing the upper margin of the D zone (Fig. 4)
5. The corresponding designed software must evaluate the optical density calculated on a grey scale obtained in the red component of the light crossing the section.
6. In order to minimise the difference of the safranin O staining between the sections and because PG content ratio parameter differentially varies during the experimental OA in U and D zones, evaluate PC as the following ratio: SOI in U zone divided by SOI in D zone.

Note 9

SBPT:

The designed software must perform an automatic segmentation of the bone in the half superior part of the epiphysis (Fig. 5).

1. Use sections stained with Goldner's trichrome at a 20× magnification.
2. Perform the segmentation of the bone using a threshold for black and white extraction on red images.
3. Isolate the bone area tangential to the growth plate extending it perpendicularly to the articular cartilage, as shown in Fig. 5.
4. The subchondral bone area can be generated automatically in the superior half above the median of the delimited rectangle (step 3).
5. Calculate the SBPT as the mean distance between each pixel of the upper limit of the bone and its corresponding point at the margin of the bone marrow.

References

1. Radin EL, Rose RM. Role of subchondral bone in the initiation and progression of cartilage damage. Clin Orthop 1986;213:34–40.
2. Dieppe PA, Cushnagan J, Young P, Kirwan JR. Prediction of the progression of joint space narrowing in osteoarthritis of the knee by bone scintigraphy. Ann Rheum Dis 1993;52:557–63.
3. Bailey AJ, Mansell JP. Do subchondral bone changes exacerbate or precede articular cartilage destruction in osteoarthritis of the elderly? Gerontology 1997;43:296–304.
4. Hunziker EB. Cartilage histomorphometry. Methods Mol Med 2007;135(1):147–66.
5. Pastoureau P, Leduc S, Chomel A, De Ceuninck F. Quantitative assessment of articular cartilage and subchondral bone histology in the meniscectomized guinea pig model of osteoarthritis. Osteoarthritis Cartilage 2003;11:412–23.
6. Pastoureau P, Chomel A. Methods for cartilage and subchondral bone histomorphometry. Methods Mol Med 2004;101:79–92.
7. Schenk RK, Olah AJ, Hermann W. Preparation of calcified tissues for light microscopy. In: Dickson GR, Ed. Methods of Calcified Tissue Preparation. Amsterdam: Elsevier Science Publisher B.V; 1984;1:1–56.
8. Oda JY, Liberti EA, Maifrino LB, de Souza RR. Variation in articular cartilage in rats between 3 and 32 months old. A histomorphometric and scanning electron microscopy study. Biogerontology 2007 Jun;8(3):345–52.
9. Hansra P, Moran EL, Fornasier VL, Bogoch ER. Carrageenan-induced arthritis in the rat. Inflammation 2000 Apr;24(2):141–55.
10. Lu JX, Prudhommeaux F, Meunier A, Sedel L, Guillemin G. Effects of chitosan on rat knee cartilages. Biomaterials 1999 Oct;20(20):1937–44.
11. Fini M, Giavaresi G, Torricelli P, Cavani F, Setti S, Canã V, *et al*. Pulsed electromagnetic fields reduce knee osteoarthritic lesion progression in the aged Dunkin Hartley guinea pig. J Orthop Res. 2005 Jul;23(4):899–908.
12. Papaioannou NA, Triantafillopoulos IK, Khaldi L, Krallis N, Galanos A, Lyritis GP. Effect of calcitonin in early and late stages of experimentally induced osteoarthritis. A histomorphometric study. Osteoarthritis Cartilage 2007 Apr;15(4):386–95.
13. Jo H, Ahn HJ, Kim EM, Kim HJ, Seong SC, Lee I, *et al*. Effects of dehydroepiandrosterone on articular cartilage during the development of osteoarthritis. Arthritis Rheum 2004 Aug;50 (8):2531–8.
14. Amiel D, Toyoguchi T, Kobayashi K, Bowden K, Amiel ME, Healey RM. Long-term effect of sodium hyaluronate (Hyalgan) on osteoarthritis progression in a rabbit model. Osteoarthritis Cartilage 2003 Sep;11(9):636–43.
15. Shimizu C, Yoshioka M, Coutts RD, Harwood FL, Kubo T, Hirasawa Y, *et al*. Long-term effects of hyaluronan on experimental osteoarthritis in the rabbit knee. Osteoarthritis Cartilage 1998 Jan;6(1):1–9.
16. Yoshioka M, Shimizu C, Harwood FL, Coutts RD, Amiel D. The effects of hyaluronan during the development of osteoarthritis. Osteoarthritis Cartilage 1997 Jul;5(4):251–60.
17. Yoshioka M, Coutts RD, Amiel D, Hacker SA. Characterization of a model of osteoarthritis in the rabbit knee. Osteoarthritis Cartilage 1996 Jun;4(2):87–98.
18. Clark AL, Leonard TR, Barclay LD, Matyas JR, Herzog W. Heterogeneity in patellofemoral cartilage adaptation to anterior cruciate ligament transection; chondrocyte shape and deformation with compression. Osteoarthritis Cartilage 2006 Feb;14(2):120–30.
19. Hwa SY, Burkhardt D, Little C, Ghosh P. The effects of orally administered diacerein on cartilage and subchondral bone in an ovine model of osteoarthritis. J Rheumatol 2001 Apr;28 (4):825–34.

20. Cake MA, Read RA, Guillou B, Ghosh P. Modification of articular cartilage and subchondral bone pathology in an ovine meniscectomy model of osteoarthritis by avocado and soya unsaponifiables (ASU). Osteoarthritis Cartilage 2000 Nov;8(6):404–11.
21. Armstrong SJ, Read RA, Price R. Topographical variation within the articular cartilage and subchondral bone of the normal ovine knee joint: a histological approach. Osteoarthritis Cartilage 1995 Mar;3(1):25–33.
22. King KB, Opel CF, Rempel DM. Cyclical articular joint loading leads to cartilage thinning and osteopontin production in a novel in vivo rabbit model of repetitive finger flexion. Osteoarthritis Cartilage 2005 Nov;13(11):971–8.
23. Daubs BM, Markel MD, Manley PA. Histomorphometric analysis of articular cartilage, zone of calcified cartilage, and subchondral bone plate in femoral heads from clinically normal dogs and dogs with moderate or severe osteoarthritis. Am J Vet Res. 2006 Oct;67(10):1719–24.
24. Oettmeier R, Arokoski J, Roth AJ, Helminen HJ, Tammi M, Abendroth K. Quantitative study of articular cartilage and subchondral bone remodeling in the knee joint of dogs after strenuous running training. J Bone Miner Res 1992 Dec;7(Suppl 2):S419–24.
25. Murray RC, Branch MV, Tranquille C, Woods S. Validation of magnetic resonance imaging for measurement of equine articular cartilage and subchondral bone thickness. Am J Vet Res. 2005 Nov;66(11):1999–2005.
26. Shimizu C, Coutts RD, Healey RM, Kubo T, Hirasawa Y, Amiel D. Method of histomorphometric assessment of glycosaminoglycans in articular cartilage. J Orthop Res. 1997 Sep;15(5):670–4.
27. Hunziker EB, Quinn TM. Surgical removal of articular cartilage leads to loss of chondrocytes from cartilage bordering the wound edge. J Bone Joint Surg Am 2003;85-A(Suppl 2):85–92.
28. Wilson D, Paul PK, Roberts ED, Blancuzzi V, Gronlund-Jacob J, Vosbeck K, *et al*. Magnetic resonance imaging and morphometric quantitation of cartilage histology after chronic infusion of interleukin 1 in rabbit knees. Proc Soc Exp Biol Med 1993 May;203(1):30–7.
29. Chateauvert JM, Grynpas MD, Kessler MJ, Pritzker KP. Spontaneous osteoarthritis in rhesus macaques. II. Characterization of disease and morphometric studies. J Rheumatol 1990 Jan;17 (1):73–83. Comment in: J Rheumatol. 1990 Jan;17(1):5–6.
30. Qin L, Zheng Y, Leung C, Mak A, Choy W, Chan K. Ultrasound detection of trypsin-treated articular cartilage: its association with cartilaginous proteoglycans assessed by histological and biochemical methods. J Bone Miner Metab 2002;20(5):281–7.
31. Fahlgren A, Messner K, Aspenberg P. Meniscectomy leads to an early increase in subchondral bone plate thickness in the rabbit knee. Acta Orthop Scand 2003 Aug;74(4):437–41.
32. Hayami T, Pickarski M, Zhuo Y, Wesolowski GA, Rodan GA. Duong le T. Characterization of articular cartilage and subchondral bone changes in the rat anterior cruciate ligament transection and meniscectomized models of osteoarthritis. Bone 2006 Feb;38(2):234–43.
33. Hayami T, Pickarski M, Wesolowski GA, McLane J, Bone A, Destefano J, *et al*. The role of subchondral bone remodeling in osteoarthritis: reduction of cartilage degeneration and prevention of osteophyte formation by alendronate in the rat anterior cruciate ligament transection model. Arthritis Rheum 2004 Apr;50(4):1193–206.
34. Brandt KD, Myers SL, Burr D, Albrecht M. Osteoarthritic changes in canine articular cartilage, subchondral bone, and synovium fifty-four months after transection of the anterior cruciate ligament. Arthritis Rheum 1991 Dec;34(12):1560–70.
35. Bendele AM, White SL. Early histopathologic and ultrastructural alterations in femorotibial joints of partial medial meniscectomized guinea pigs. Vet Pathol 1987;24:436–43.
36. Wang SX, Laverty S, Dumitriu M, Plaas A, Grynpas MD. The effects of glucosamine hydrochloride on subchondral bone changes in an animal model of osteoarthritis. Arthritis Rheum 2007;56(5):1537–48.
37. Gundersen HJ, Bagger P, Bendtsen TF, Evans SM, Korbo L, Marcussen N, *et al*. The new stereological tools: dissector, fractionator, nucleator and point sampled intercepts and their use in pathological research and diagnosis. APMIS 1988;96(10):857–81.
38. Pelletier JP, Martel-Pelletier J, Howell DS. Etiopathogenesis of osteoarthritis. In: Koopman WJ, Ed. Arthritis and allied conditions. A textbook of Rheumatology. 13th edn. Baltimore: Williams and Wilkins; 1997:1969–84.
39. Hunziker EB, Graber W. Differential extraction of proteoglycans from cartilage tissue matrix compartments in isotonic buffer salt solutions and commercial tissue-culture media. J Histochem Cytochem 1986;34(9):1149–53.
40. Engfeldt B, Hjertquist SO. Studies on the epiphyseal growth zone. Virchows Archive 1968;1:222–9.
41. Hunziker EB, Herrmann W, Schenk RK. Improved cartilage fixation by ruthenium hexammine trichloride (RHT). A prerequisite for morphometry in growth cartilage. J Ultrastruct Res. 1982;81(1):1–12.
42. Hunziker EB, Herrmann W, Schenk RK. Ruthenium hexammine trichloride (RHT)-mediated interaction between plasmalemmal components and pericellular matrix proteoglycans is responsible for the preservation of chondrocytic plasma membranes in situ during cartilage fixation. J Histochem Cytochem 1983;31(6):717–27.
43. Sandell LJ, Aigner T. Articular cartilage and changes in arthritis. An introduction: cell biology of osteoarthritis. Arthritis Res 2001;3(2):107–13.
44. Karsdal MA, Leeming DJ, Dam EB, Henriksen K, Alexandersen P, Pastoureau P, *et al*. Review: should subchondral bone turnover be targeted when treating osteoarthritis? Osteoarthritis Cartilage 2008;16(6):638–46.
45. Smith MM. Pathobiology of the synovium in osteoarthritis. APLAR Journal of Rheumatology 2002;5(1):A1–A10.
46. O'Driscoll SW, Marx SG, Fitzsimmons JS, Beaton DE. Method for automated cartilage histomorphometry. Tissue Eng 1999;5 (1):13–23.
47. Hacker SA, Healey RM, Yoshioda M, Coutts RD. A methodology for the quantitative assessment of articular cartilage histomorphometry. Osteoarthritis Cartilage 1997;5(5):343–55.
48. Sabatini M, Lesur C, Thomas M, Chomel A, Anract P, de Nanteuil G, *et al*. Effect of inhibition of metalloproteinases on cartilage loss in vitro and in guinea pig model of osteoarthritis. Arthritis Rheum 2005;52(1):171–80.